Limnol. Oceanogr., 57(5), 2012, 1266–1278

doi:10.4319/lo.2012.57.5.1266

Temperature, resources, and phytoplankton size structure in the ocean

Emilio Marañón,[a,*] Pedro Cermeño,[a] Mikel Latasa,[b] and Rémy D. Tadonléké[c]

[a] Departamento de Ecoloxía e Bioloxía Animal, Universidade de Vigo, Vigo, Spain
[b] Instituto Español de Oceanografía, Centro Oceanográfico de Gijón, Gijón, Spain
[c] Institut National de la Recherche Agronomique, Station d'Hydrobiologie Lacustre, Thonon les Bains, France

Abstract

We conducted a meta-analysis of temperature, phytoplankton size structure, and productivity in cold, temperate, and warm waters of the world's oceans. Our data set covers all combinations of temperature and resource availability, thus allowing us to disentangle their effects. The partitioning of biomass between different size classes is independent of temperature, but depends strongly on the rate of resource use as reflected in the rate of primary production. Temperature and primary production explained 2% and 62%, respectively, of the variability in the contribution of microphytoplankton to total biomass. This contribution increases rapidly with total biomass and productivity, reaching values $> 80\%$ when chlorophyll *a* concentration is > 2 μg L^{-1} or primary production is > 100 μg C L^{-1} d^{-1}, irrespective of water temperature. Conversely, picophytoplankton contribution is substantial ($> 40\%$), at all temperatures, only when chlorophyll *a* concentration is < 1 μg L^{-1} or primary production is < 50 μg C L^{-1} d^{-1}. The temperature–size rule cannot explain these changes, which instead reflect fundamental reorganizations in the species composition of the assemblage, arising from taxon- and size-dependent differences in resource acquisition and use. Given that resource availability, rather than temperature per se, is the key factor explaining the relative success of different algal size classes, there will be no single, universal effect of global warming on phytoplankton size structure.

Phytoplankton size structure largely determines the trophic organization of pelagic ecosystems and thus the efficiency with which organic matter produced by photosynthesis is channeled towards upper trophic levels or exported to the ocean's interior (Legendre and Rassoulzadegan 1996; Falkowski and Oliver 2007; Finkel et al. 2010). The dominance, in terms of biomass and production, by small phytoplankton is associated with slow sedimentation rates and intense recycling of matter through the microbial food web, which results in little potential for carbon export. In contrast, dominance by large species allows a more efficient transfer of organic matter through short food chains towards upper trophic levels, as well as enhanced downward export fluxes and biological CO_2 drawdown. Marine phytoplankton are responsible for almost half of global primary production and, due to their fast turnover times, have the potential to respond rapidly to alterations in environmental forcing (Falkowski et al. 1998). Yet it is not clear how different global change processes, involving temperature and resource supply among other factors, will affect phytoplankton size structure and associated functional properties.

Smaller phytoplankton cells, due to a higher surface-area-to-volume ratio and a smaller thickness of the diffusion boundary layer, have competitive advantage over larger cells in nutrient-impoverished environments (Chisholm 1992; Kiørboe 1993; Raven 1998). Conversely, larger phytoplankton are capable of sustaining higher rates of biomass-specific production rates in nutrient-rich waters (Cermeño et al. 2005; Marañón et al. 2007) and, in addition, are less tightly controlled by grazers (Kiørboe 1993). In principle, these constraints would explain the fact that the picophytoplankton (cells of < 2 μm in diameter) dominate the autotrophic biomass and production of oligotrophic regions, whereas microphytoplankton (cells of > 20 μm in diameter) dominate in productive areas (Chisholm 1992; Agawin et al. 2000; Marañón et al. 2001). However, temperature and nutrient supply are strongly anticorrelated in the ocean (Kamykowski and Zentara 1986) and therefore separating the role of these two factors has proven to be difficult (Agawin et al. 2000).

Several studies have recently suggested a direct and important effect of temperature on the size structure of phytoplankton assemblages, such that warmer temperatures would cause an increased contribution of small cells to total phytoplankton biomass. Morán et al. (2010) reported that 73% of the variability in the contribution of picophytoplankton to total phytoplankton biomass in temperate waters of the North Atlantic is explained by temperature alone, irrespective of trophic status and resource supply as inferred from in situ nutrient concentrations. These authors explained their findings as a result of the temperature–size rule for protists (Atkinson et al. 2003), which predicts a decrease in the intraspecific, mean cell size as temperature warms. Using data collected during a circumnavigation of all major ocean basins, Hilligsøe et al. (2011) reported that the inverse relationship between the percentage of > 10 μm chlorophyll *a* (Chl *a*) and temperature had the same slope in samples of high and low nutrient concentration. From this observation, Hilligsøe et al. (2011) concluded that temperature directly affects phytoplankton size structure. The decrease in body size has been termed the third universal ecological response to global warming in aquatic ecosystems, in addition to changes in species distribution and phenology (Daufresne et al. 2009). However, before concluding that this so-called

* Corresponding author: em@uvigo.es

Table 1. Details of the studies from which the data of Chl *a* concentration in pico-, nano-, and microphytoplankton were obtained. *n* indicates the number of data points for each study. For full references *see* Web Appendix, www.aslo.org/lo/toc/vol_57/issue_5/1266a.pdf.

Program	Location	Latitude	Longitude	Sampling period	*n*	Reference
Atlantic Meridional Transect	Atlantic Ocean	49°N–52°S	58°W–14°W	Apr–May and Oct–Nov 1996	236	Marañón et al. 2001
Tamaño, Producción y Respiración del Fitoplancton (TPR) project	Ría de Vigo (northwest Iberian peninsula)	42°14′N	8°47′W	Jul 2001–Jul 2002	66	Cermeño et al. 2006
SEEDS	Western subarctic North Pacific	48.5°N	165°E	Jul 2001	47	Tsuda et al. 2003
SOIREE	Southern Ocean	61°S	140°E	Feb 1999	46	Boyd et al. 2000
U.S. Joint Global Ocean Flux Study (JGOFS) Arabian Sea Process Study	Arabian Sea	10°N–19°N	57°E–67°E	Mar–Nov 1995	61	Latasa and Bidigare 1998
Rothera Time Series	Marguerite Bay, western Antarctic Peninsula	67°34′S	68°13′W	Jul 2003–Jul 2004	44	Clarke et al. 2008

universal rule applies to phytoplankton, the effects of temperature and resource supply on phytoplankton size structure must be separated. If temperature does play a direct role (e.g., not through its relationship with nutrient or light availability) in the control of phytoplankton size structure in the ocean, this should be made evident through the analysis of a sufficiently large data set including observations of all combinations of temperature and resource supply conditions.

Here we conduct a meta-analysis of published data of phytoplankton size structure obtained in cold, temperate, and warm waters from coastal and open-ocean regions throughout the world. In order to separate the effect of temperature and resource supply, we searched for studies conducted in environments where phytoplankton biomass and productivity change widely while temperature remains relatively constant. We also searched for measurements conducted in settings where cold temperatures coincide with low resource supply, or where warm temperatures coincide with high resource supply. Our goal is to test the hypothesis that temperature per se (e.g., not through indirect effects related to nutrient or light availability) plays a role in the control of phytoplankton size structure in the ocean.

Methods

To determine the relationship between total phytoplankton biomass and the relative importance of different phytoplankton size classes, we compiled measurements of size-fractionated Chl *a* concentration in the euphotic layer from different marine research programs (Table 1). Size-fractionated Chl *a* was measured fluorometrically after sequential filtration of samples through nylon or polycarbonate filters of 20-, 2-, and 0.2-μm pore size (Whatman GF/F filters were sometimes used instead of 0.2-μm polycarbonate filters), which allows the determination of microphytoplankton ($>$ 20 μm), nanophytoplankton (2–20 μm), and picophytoplankton (0.2–2 μm) Chl *a*. In the case of the Subarctic Pacific Iron Experiment for Ecosystem Dynamics Study (SEEDS) cruise, 10-μm filters instead of 20-μm filters were used to separate the largest size fraction. Total Chl *a* was calculated as the sum of the Chl *a* in each size class. The resulting data set contains 500 measurements of size-fractionated Chl *a* conducted in polar, subpolar, temperate, subtropical, and tropical regions of the ocean.

To analyze the relationship between phytoplankton size structure, temperature, and primary production, we used only surface (0–40 m and 0–15 m for open-ocean and coastal waters, respectively) data so as to avoid the confounding effect of vertical variability. For instance, in tropical and subtropical waters, large temperature changes can occur between the surface and the base of the euphotic layer, while phytoplankton size structure remains virtually unchanged (Marañón et al. 2001). Similarly, an equally low primary production rate can be measured in surface waters of an oligotrophic region or at the base of the euphotic layer in a highly productive area. From the original data set of 500 measurements, we thus selected 224 concurrent measurements of surface temperature and size-fractionated Chl *a*. We also searched the literature for additional records of temperature and size-fractionated Chl *a* in surface or near-surface waters. In particular, we looked for gradients in temperature that were not associated with changes in phytoplankton biomass and productivity, and vice versa, in order to disentangle the effect of temperature and resource supply. Data were obtained directly from the authors or extracted from the publications. We thus obtained a data set of 330 concurrent measurements of surface temperature and size-fractionated Chl *a*, of which 165 were also accompanied by determinations of primary production (Table 2). Primary production requires a supply of nutrients and light and therefore its rate is an indicator of resource utilization rate by phytoplankton. Primary production was measured by determining the uptake rate of dissolved inorganic carbon, labeled with ^{14}C or ^{13}C, during in situ or on-deck incubations. All data sets used in the present analysis are available from the authors upon request.

Table 2. Details of the studies from which surface temperature, size-fractionated Chl *a* concentration, and, where available, primary production data were obtained. *n* indicates the number of data points from each data subset used to compute the mean and standard deviation values shown in Fig. 5. The label identifies each data subset in Fig. 5. HNLC: high-nutrient, low-chlorophyll; na: not available. For full references *see* Web Appendix.

Program	Location	Latitude	Longitude	Sampling period	Subset	*n*	Label	Reference
Rothera Time Series	Marguerite Bay, west Antarctic Peninsula	67°S	68°W	Jul–Sep 2003	Winter	8	*1*	Clarke et al. 2008
				Jan–Mar 2004	Summer	15	*2*	
Scandinavia–South Africa Antarctic cruise	Southern Ocean, east Atlantic sector	61°S–57°S	6°E	Dec 1997–Jan 1998	Spring ice edge	6	*3*	Froneman et al. 2004
South African Antarctic Marine Ecosystems Study	Southern Ocean, east Atlantic sector	67°S–63°S	0°E	Jan–Feb 1993	Marginal ice zone	4	*4*	Froneman et al. 2001
		56°S–45°S	0°E–10°E	Jan–Feb 1993	Antarctic polar front	8	*5*	
SOIREE	Southern Ocean, Australian sector	61°S	140°E	Feb 1999	Inside	15	*6*	Boyd et al. 2000
				Feb 1999	Outside	16	*7*	
SOFeX	Southern Ocean, Pacific sector	56°S	172°W	Jan 2002	Inside	na	*8*	Lance et al. 2007
				Jan 2002	Outside	na	*9*	
Kerguelen Ocean and Plateau compared Study	Kerguelen Plateau	50°S	72°E	Jan–Feb 2005	Bloom area	4	*10*	Christaki et al. 2008
		52°S	77°E	Jan–Feb 2005	HNLC area	2	*11*	
SEEDS	Northwest subarctic Pacific	48°N	165°E	Jul 2001	Inside	12	*12*	Tsuda et al. 2003
				Jul 2001	Outside	10	*13*	
SERIES	Northeast subarctic Pacific	50°N	144°W	Jul–Aug 2002	Inside	6	*14*	Marchetti et al. 2006
				Jul–Aug 2002	Outside	5	*15*	
R/V *Kaiyo Maru* cruise	Okhotsk Sea, west Pacific Ocean	45°N–50°N	145°E–152°E	Oct 1993	Late autumn	9	*16*	Shiomoto 1997
				Nov 1993	Early winter	9	*17*	
Canadian JGOFS Subarctic Pacific study	Northeast subarctic Pacific	49°N–50°N	125°W–145°W	Sep 1992, Sep 1995, Sep 1996	Late summer	15	*18*	Boyd and Harrison 1999
				Mar 1993, Feb 1996, Feb 1997	Late winter	12	*19*	
				May 1993, May 1996, June 1997	Late spring	15	*20*	
Station KNOT time series	Northwest subarctic Pacific	44°N	155°W	Jun, Jul, Aug 1998	Summer	4	*21*	Imai et al. 2002
				Oct 1998	Autumn	2	*22*	
				Jan, Feb 1999	Winter	2	*23*	
TPR project	Ría de Vigo (northwest Iberia)	42°N	9°W	Nov–Dec 2001 and Jan 2002	Winter	6	*24*	Cermeño et al. 2006
				Apr–Jul 2002	Upwelling season	12	*25*	
Tehuanos II	Tehuantepec Gulf, southwest Mexico	15°N–18°N	95°W–105°W	Jan, Feb 1999	Winter 1999	4	*26*	Lara-Lara and Bazán-Guzmán 2005

Table 2. Continued.

Program	Location	Latitude	Longitude	Sampling period	Subset	*n*	Label	Reference
Tehuanos II	Tehuantepec Gulf, southwest Mexico	15°N	96°W	Jan, Feb 1989	Winter 1989	3	*27*	Robles-Jarero and Lara-Lara 1993
Johor Strait survey	Johor Strait, Singapore	1°N	104°W	May, Jul 1998	Sta. E3	3	*28*	Gin et al. 2000
Iskenderun Bay survey	Iskenderun Bay, northeast Mediterranean Sea	36°N	35°E	Jul 2003	Sta. 2, 3, 4, and 5	4	*29*	Polat and Aka 2007
Atlantic Meridional Transect	Atlantic Ocean	40°N–10°N 10°S–40°S	53°W–20°W	May and Oct 1996	Subtropical gyres	23	*30*	Marañón et al. 2001
U.S. JGOFS Arabian Sea Process Study	Arabian Sea	10°N–19°N	57°E–67°E	Mar–Nov 1995	Monsoon	10	*31*	Latasa and Bidigare 1998
IronEx II	Eastern Equatorial Pacific	4°S	105°W	Jun 1995	Inside	4	*32*	Cavender-Bares et al. 1999
				Jun 1995	Outside	4	*33*	

We used simple and multiple regression analysis to assess the relative importance of temperature and resource use rate (represented by the rate of primary production) in the control of phytoplankton size structure. These analyses were carried out using the ensemble of samples ($n = 165$) for which concurrent data of temperature, primary production, and size-fractionated Chl *a* concentration were available. To attain homoscedasticity, primary production data were $\log_{10}$-transformed prior to analysis. In multiple regression analysis, we calculated the squared semi-partial correlation coefficients, which indicate the proportion of unique variance in the dependent variable that is accounted for by each independent variable.

Results

Size-fractionated vs. total phytoplankton biomass—The biomass of each phytoplankton size class, as estimated from Chl *a* concentration, describes contrasting patterns as total phytoplankton biomass increases (Fig. 1). Picophytoplankton Chl *a* increases up to ca. 0.5 μg L^{-1} and then decreases, whereas microphytoplankton Chl *a* continues to increase even when total Chl *a* is very high. Nanophytoplankton Chl *a* reaches larger levels than picophytoplankton but rarely gets higher than 1 μg L^{-1}. Microphytoplankton show the largest range of variability in Chl *a* concentration ($>$ 4 orders of magnitude), whereas nanophytoplankton show the narrowest (2 orders of magnitude). When Chl *a* concentration is below 0.5 μg L^{-1}, picophytoplankton and, occasionally, nanophytoplankton are the dominant size class. In contrast, when Chl *a* concentration is above 1 μg L^{-1}, microphytoplankton show an overwhelming dominance of total photosynthetic biomass. These patterns are also present when the data are separated by temperature (Fig. 2). The dominance of microphytoplankton at high biomass levels occurs both in cold (< 10°C) and temperate (10–20°C) waters, while the dominance of picophytoplankton at low biomass levels can be seen in both temperate and warm (> 20°C) waters.

The variability in the relative importance of each size class as total phytoplankton biomass changes is best visualized by plotting the percentage of Chl *a* in a given size class against total Chl *a* concentration (Fig. 3). The relative contribution of picophytoplankton shows a strong inverse relationship with total phytoplankton biomass, with values of up to $> 90\%$ when total Chl *a* is below 1 μg L^{-1} (Fig. 3A). At total Chl *a* levels above 1 μg L^{-1}, picophytoplankton typically contributes $< 10\%$ of total phytoplankton biomass, both in temperate and warm waters. The nanophytoplankton size class shows a similar pattern of increasing relative importance with decreasing total Chl *a* levels, although only on a small fraction of samples accounting for more than 60% of total phytoplankton biomass (Fig. 3B). A relatively high (e.g., $> 50\%$) contribution of nanophytoplankton at low total Chl *a* levels occurs in temperate and cold waters, but not in warm waters, where this size class tends to account for 5–40% of total phytoplankton biomass. Finally, the relative importance of microphytoplankton increases rapidly with increasing total Chl *a* in cold, temperate, and warm waters,

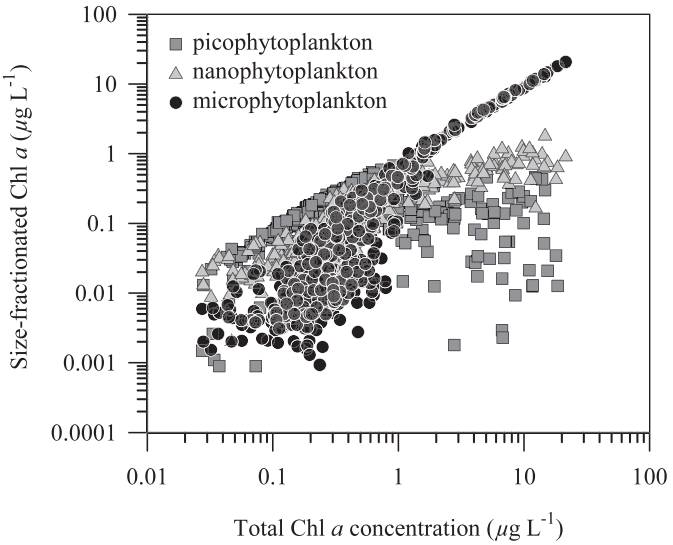

Fig. 1. Total chlorophyll *a* (Chl *a*) concentration vs. Chl *a* concentration in picophytoplankton (0.2–2 μm), nanophytoplankton (2–20 μm), and microphytoplankton (> 20 μm).

and reaches values > 80% when total Chl *a* is above 2–3 μg L^{-1}, both in cold and temperate waters (Fig. 3C).

Temperature and phytoplankton size structure—The patterns shown on Figs. 1–3 indicate that phytoplankton size structure depends strongly on total phytoplankton biomass and, furthermore, suggest that this dependence occurs irrespective of temperature. However, to examine closely the relationship between temperature and size structure, we analyzed the contribution of each size class to total Chl *a* as a function of temperature (Fig. 4), using the data sets described in Table 2. We found no relationship between temperature and phytoplankton size structure, as the relative contribution of each size class to total Chl *a* can take virtually any value at all temperature ranges (Fig. 4). The percentage of Chl *a* in pico- and microphytoplankton varied between 0–80% and 0–90%, respectively, across the whole temperature range (Fig. 4A,C). Nanophytoplankton contribution to total Chl *a* generally ranged between 0–60% at all temperatures, but showed some values between 60–80% at very cold temperatures (Fig. 4B). Examining the mean values of temperature and the percentage of Chl *a* in the microphytoplankton size class at different locations and/or time periods indicates that, in both coastal and oceanic regions, and for cold, temperate, and warm waters, totally different phytoplankton size structures can be found with little or no change in temperature (Fig. 5).

In Marguerite Bay (western Antarctic peninsula), the contribution of microphytoplankton to total Chl *a* changed from 15% in winter to 89% in summer (data sets 1 and 2, respectively, in Fig. 5 and Table 2), with a concurrent temperature change of 2.5°C. In the eastern Atlantic sector of the Southern Ocean, the percentage of microphytoplankton Chl *a* changed from 7% in the Antarctic polar front (data set 5) to 61% in the marginal ice zone (data set 4), with an associated temperature decrease of 4°C. During

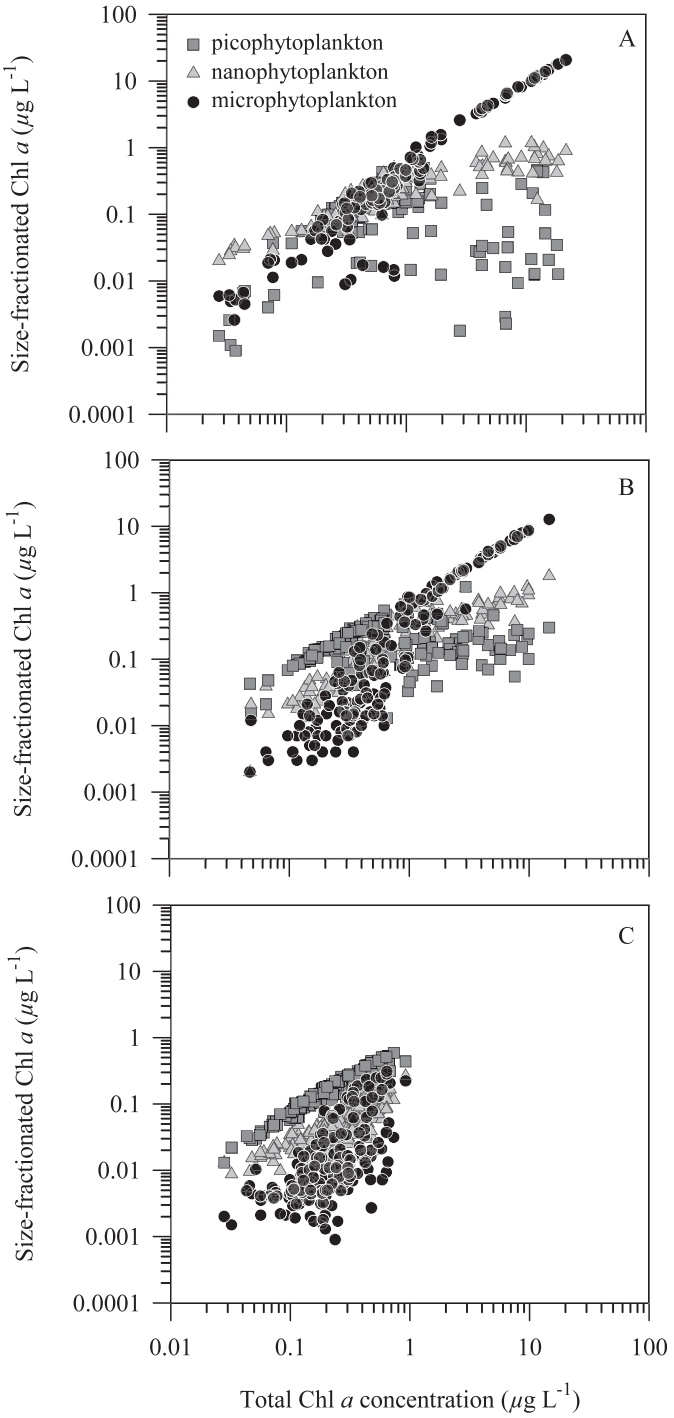

Fig. 2. Total Chl *a* concentration vs. Chl *a* concentration in picophytoplankton (0.2–2 μm), nanophytoplankton (2–20 μm), and microphytoplankton (> 20 μm) for (A) cold (< 10°C), (B) temperate (10–20°C), and (C) warm (> 20°C) waters.

in situ iron addition experiments, large increases in the relative importance of microphytoplankton took place in the fertilized waters without any change in temperature. Shown on Fig. 5 are data from inside and outside the fertilized patch during the Southern Ocean Iron Release Experiment (SOIREE), the Southern Ocean Iron Experiment

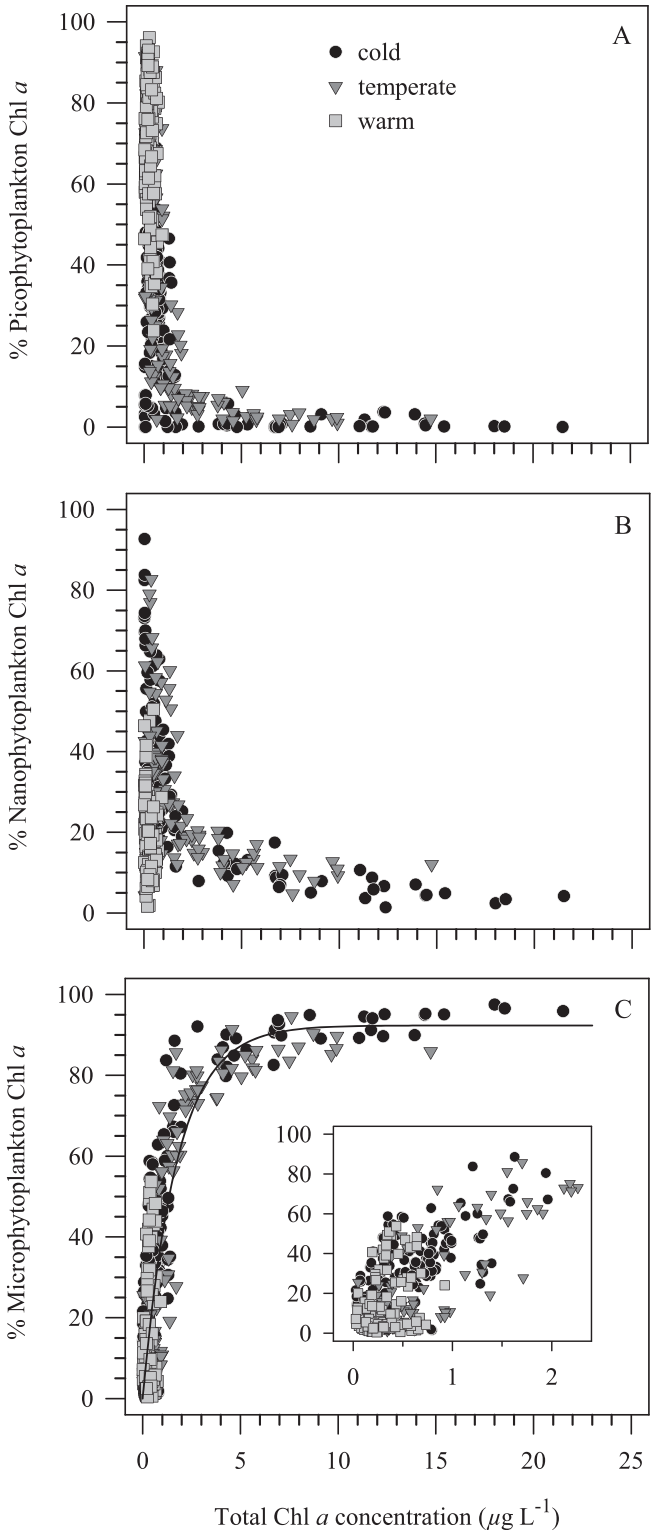

Fig. 3. Total Chl *a* concentration vs. the contribution of (A) picophytoplankton, (B) nanophytoplankton, and (C) microphytoplankton to total Chl *a* in cold (< 10°C), temperate (10–20°C), and warm (> 20°C) waters. (C) The inset shows the data with total Chl *a* concentration below 2.5 μg L^{-1}. The fitted line is $y = 92.3(\pm 2.2)(1 - \exp(-53.4(\pm 1.9)x/92.3(\pm 2.2)))$, $r^2 = 0.78$, $p < 0.001$, $n = 500$.

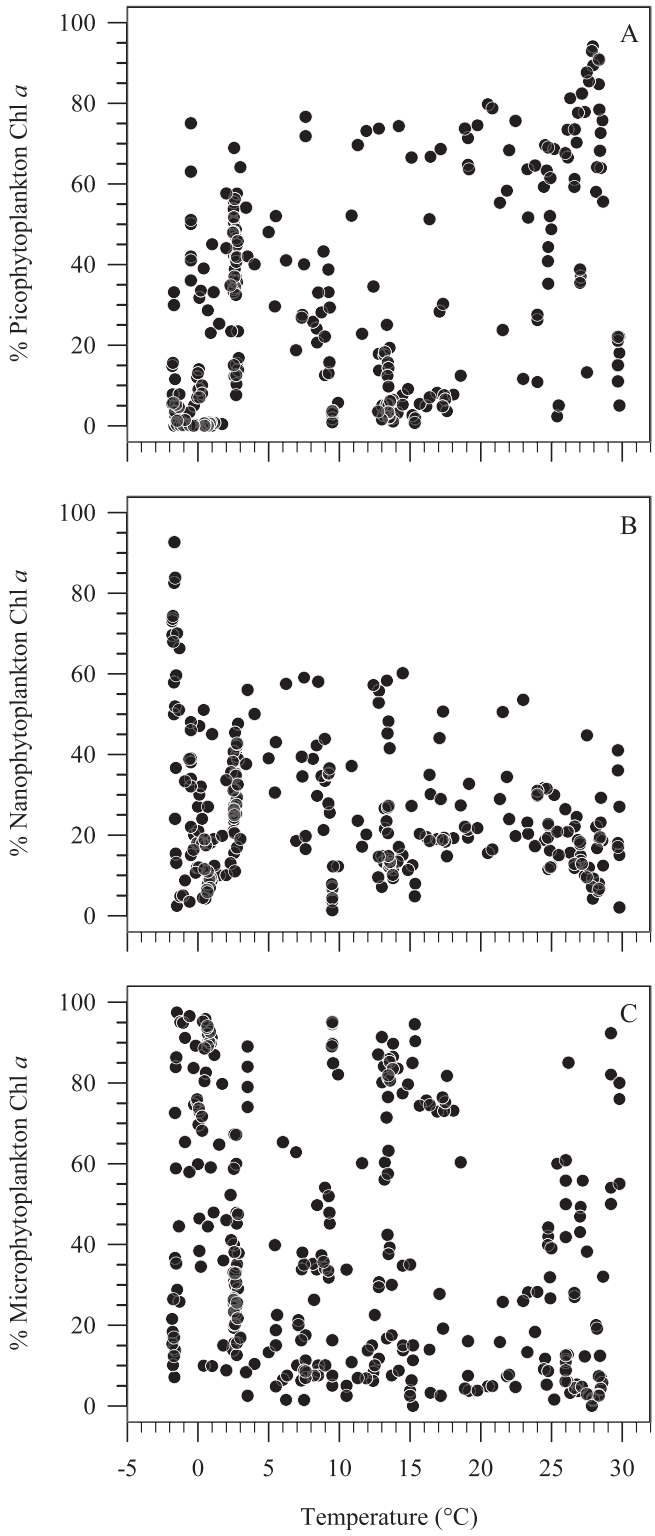

Fig. 4. Temperature vs. the contribution of (A) picophytoplankton, (B) nanophytoplankton, and (C) microphytoplankton to total Chl *a* concentration.

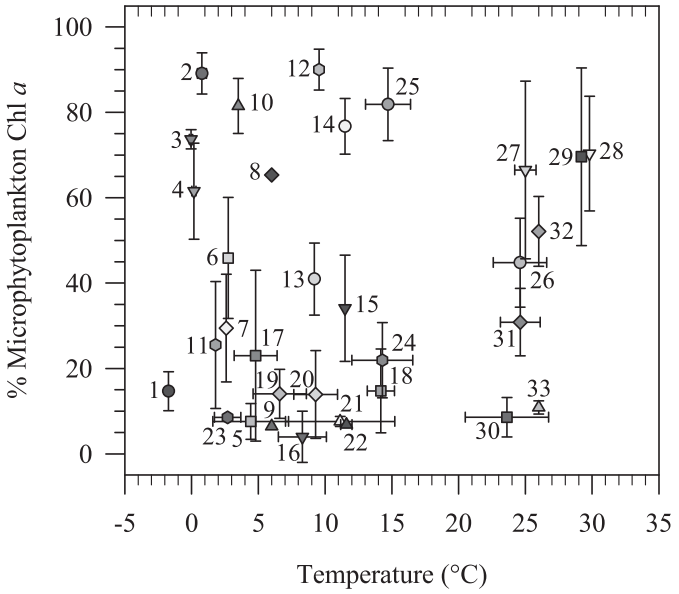

Fig. 5. Mean (± standard deviation) temperature vs. microphytoplankton contribution to total Chl *a* in different locations of the world's oceans: Marguerite Bay (western Antarctic Peninsula) in (1) July–September 2003 and (2) January–March 2004; (3) the spring ice edge zone in the eastern Atlantic sector of the Southern Ocean in December 1997–January 1998; (4) the marginal ice zone and (5) the Antarctic polar front in the eastern Atlantic sector of the Southern Ocean in January–February 1993; (6) inside and (7) outside the fertilized patch during the SOIREE iron addition experiment in the Southern Ocean; (8) inside and (9) outside the north fertilized patch during the SOFeX iron addition experiment in the Southern Ocean; (10) inside and (11) outside a naturally iron-fertilized area in the Kerguelen Plateau (Southern Ocean) during the Kerguelen Ocean and Plateau compared Study (KEOPS); (12) inside and (13) outside the fertilized patch during the SEEDS iron addition experiment in the western subarctic Pacific Ocean; (14) inside and (15) outside the fertilized patch during the SERIES iron addition experiment in the Gulf of Alaska (eastern subarctic Pacific Ocean); the Okhotsk Sea (western Pacific Ocean) in (16) October 1993 and (17) November 1993; the northeast subarctic Pacific in (18) late summer, (19) late winter, and (20) late spring; the northwest subarctic Pacific in (21) summer, (22) autumn, and (23) winter; the Ría de Vigo (northwest Iberian peninsula) during (24) winter and (25) the upwelling season; the Gulf of Tehuantepec (southwest Mexico) in (26) January–February 1999 and (27) January–February 1989; (28) eastern Johor Strait (Singapore) in May and July 1998; (29) Iskenderun Bay (northeastern Mediterranean Sea) in July 2003; (30) the north and south Atlantic subtropical gyres in April and October 1996; (31) the Arabian Sea during the 1995 monsoon (August–September); (32) inside and (33) outside the fertilized patch during the IronEx II iron addition experiment in the Equatorial Pacific. *See* Table 2 for details on each data set.

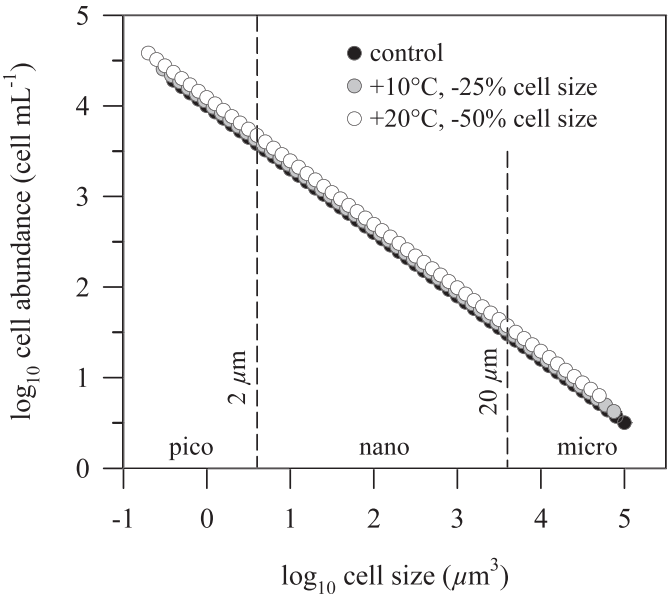

Fig. 6. Cell size vs. population abundance in a hypothetical phytoplankton assemblage composed of 55 species. Filled circles represent the original assemblage, gray symbols correspond to an assemblage in which the cell size of each species has decreased by 25% (associated with a 10°C temperature increase), and open circles correspond to an assemblage in which the cell size of each species has decreased by 50% (associated with a 20°C temperature increase). *See* Results for details on calculations.

(SOFeX), the SEEDS, the Subarctic Ecosystem Response to Iron Enrichment Study (SERIES), and the second Equatorial Pacific Iron Enrichment Experiment (IronExII). The percentage of microphytoplankton Chl *a* increased from 29% to 46% in SOIREE (data sets 7 and 6, respectively), from 6% to 65% in SOFeX (data sets 9 and 8), from 41% to 90% in SEEDS (data sets 13 and 12), from 34% to 77% in SERIES (data sets 15 and 14), and from 11% to 52% in IronExII (data sets 33 and 32). Similarly, microphytoplankton Chl *a* inside a naturally iron-fertilized area in the Kerguelen Plateau contributed 81% of total Chl *a*, compared with 25% in non-fertilized waters, which were 2.5°C warmer (data sets 10 and 11). In the temperate, coastal waters of Ría de Vigo (northwest Iberian peninsula), the contribution of microphytoplankton to total Chl *a* was 22% in winter and 82% during the upwelling season, while the mean temperature in these two periods differed by < 0.5°C (data sets 24 and 25). There were also instances of relatively constant size structure in spite of marked changes in temperature. For example, the mean temperature on a transect of five stations in the northeast subarctic Pacific was 14°C in summer and 6°C in winter, while the mean microphytoplankton contribution to total Chl *a* was 14% in both seasons (data sets 18 and 19). Similarly, the mean temperature at Kyodo North Pacific Ocean Time-series (KNOT) station in the northwest subarctic Pacific was 11°C in summer and 3°C in winter, while the percentage of microphytoplankton Chl *a* was 8% in both time periods (data sets 21 and 23). Finally, contrasting phytoplankton size structures are also observed in warm waters with similar temperatures. In the north and south Atlantic subtropical gyres, the mean microphytoplankton contribution to total Chl *a* was 8% and the mean temperature was 24°C (data set 30), but in the Arabian Sea during the monsoon period the corresponding figures were 31% and 25°C (data set 31). A strong dominance of microphytoplankton, with a relative contribution to total Chl *a* of

around 70%, was observed in warm (25–30°C), coastal waters of Tehuantepec Gulf (southwest Mexico), Iskenderun Bay (northeast Mediterranean Sea), and the eastern Johor Strait (Singapore) (data sets 27–29).

Effect of the temperature–size rule on the size–abundance distribution—We conducted a simulation to estimate the effect that temperature-driven changes in intraspecific mean cell size may have on phytoplankton size structure and the partitioning of biomass among different size classes. We consider a hypothetical phytoplankton assemblage composed of 55 species ranging in cell volume (V) from 0.4 to 10^5 μm^3 (Fig. 6). From each species to the next along the size spectrum, V increases by a factor of $10^{0.1}$. The abundance of each species scales as $V^{-0.7}$, such that the linear relationship between the logarithms of abundance and cell size (the size–abundance spectrum [SAS]) has a slope of −0.7. This slope value is typical of coastal, productive waters where nano- and microphytoplankton are dominant in terms of biomass (Reul et al. 2005; Marañón et al. 2007). Experimental evidence indicates that, in unicellular protists, the mean intraspecific cell volume decreases by ca. 2.5% for each °C of temperature increase (Atkinson et al. 2003). We thus applied a reduction of 25% and 50% to each species' cell volume, corresponding with a warming of 10°C and 20°C, respectively. In each case we adjusted the value of the SAS intercept to ensure that total biovolume of each species, and therefore the whole assemblage, remained constant. As a result of the reduction in cell volume, the abundance of all species increases and the SAS is shifted upwards and towards the left (Fig. 6). In our particular example, the partitioning of biomass (biovolume) among pico-, nano-, and microphytoplankton was 2.6%, 34.0%, and 63.4%, respectively, for the original (control) assemblage. After a 25% reduction in cell volume (associated with a 10°C warming), the contribution of pico-, nano-, and microphytoplankton to total biovolume became, respectively, 3.0%, 36.4%, and 60.6%. For a 50% reduction in cell volume (20°C warming), the corresponding figures were 3.7%, 41.8%, and 54.4%. The temperature–size rule, therefore, can only cause very minor changes in phytoplankton size structure.

Resource utilization rate and phytoplankton size structure—The strong relationship between total Chl *a* concentration and its partitioning between different size classes already suggests that the rate of resource utilization is the main factor controlling phytoplankton size structure in the ocean. Phytoplankton have fast turnover rates, ranging from a few hours to a few days, and therefore the variability in their standing stocks largely reflects the variability in the rate at which resources, light and nutrients, are used to synthesize new biomass (Irwin and Finkel 2008). However, hydrodynamic processes can also lead to the accumulation and dispersion of cells, and trophic loss processes such as grazing and viral lysis also affect phytoplankton biomass variability. To determine if there is a connection between resource utilization and phytoplankton size structure, we represented the relative contribution of each size class to total Chl *a* concentration against the rate of primary production

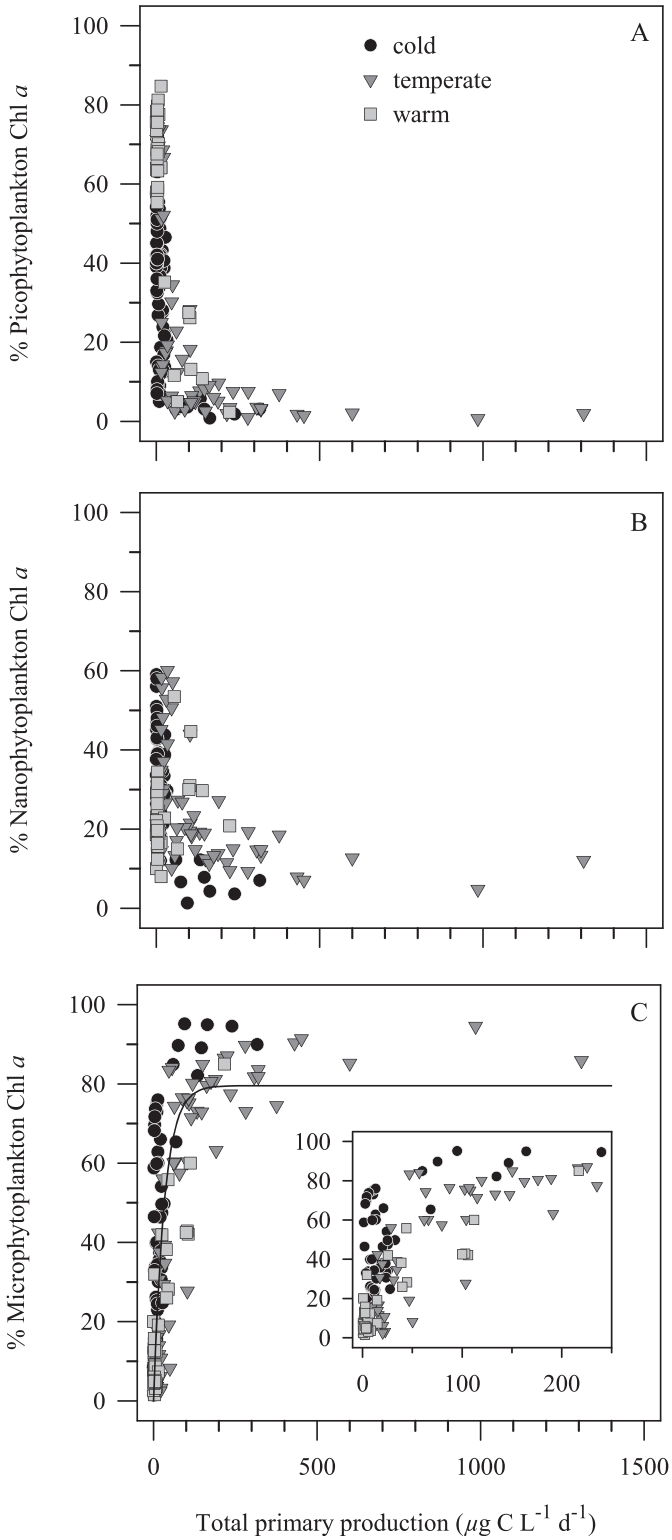

Fig. 7. Total primary production vs. the contribution of (A) picophytoplankton, (B) nanophytoplankton, and (C) microphytoplankton to total Chl *a* concentration in cold (< 10°C), temperate (10–20°C), and warm (> 20°C) surface waters. (C) The inset shows the data with primary production rates below 250 μg C L^{-1} d^{-1}. The fitted line is $y = 79.5(\pm 2.3)(1 - \exp(-2.4(\pm 0.3)x/79.5(\pm 2.3)))$, $r^2 = 0.59$, $p < 0.001$, $n = 165$.

Table 3. Results of simple linear regression analysis on the percentage of Chl *a* in each size fraction (picophytoplankton [pico], nanophytoplankton [nano], and microphytoplankton [micro]) using temperature and primary production as independent variables. Primary production data were $\log_{10}$-transformed prior to analysis. In all cases, $n = 165$.

Dependent variable	Independent variable	Slope (standard error)	Intercept (standard error)	r^2	p
% pico Chl *a*	Temperature	0.81(0.22)	24.72(3.48)	0.07	0.0004
	Primary production	−23.97(1.79)	63.51(2.57)	0.52	<0.0001
% nano Chl *a*	Temperature	−0.31(0.11)	29.80(1.72)	0.04	0.0063
	Primary production	−6.13(1.17)	33.19(1.68)	0.14	<0.0001
% micro Chl *a*	Temperature	−0.51(0.27)	45.47(4.13)	0.02	0.0600
	Primary production	30.10(1.85)	3.30(2.65)	0.62	<0.0001

(Fig. 7), which is a proxy for the rate of resource utilization. We found that, as shown before for the relationship between size-fractionated Chl *a* and total Chl *a* (Fig. 3), phytoplankton size structure is strongly related to total primary production. We also found that this relationship is present at all temperature ranges. At intermediate and high levels of primary production, the relative contribution of picophytoplankton to total Chl *a* is always below 10%, whereas it increases to values > 40% when primary production is below 100 μg C L^{-1} d^{-1}, irrespective of temperature (Fig. 7A). Nanophytoplankton contribution also tends to increase as primary production decreases (Fig. 7B). In contrast, microphytoplankton contribution increases rapidly with primary production, reaching values above 60% when carbon fixation is above 100 μg C L^{-1} d^{-1} (Fig. 7C). The same trend of increasing importance of microphytoplankton biomass with increasing primary production is observed in cold, temperate, and warm waters.

Temperature vs. resource use rate as controls of phytoplankton size structure—Simple linear regression analysis indicates that the rate of resource use, as estimated from primary production rate, explains a much larger amount of variance in size-fractionated Chl *a* than temperature does (Table 3). As shown above (Fig. 3), pico- and microphytoplankton are the size classes with a larger range of variability in their contribution to total biomass. The amount of variability explained by primary production rate for these size fractions was 52% and 62%, respectively, compared with 7% and 2% that was explained by temperature. Similarly, multiple regression analysis indicated that primary production explains 57% and 65% of the variability in the percentage of Chl *a* in pico- and microphytoplankton, respectively, whereas temperature only explains 12% and 5% (Table 4). It must be noted, however, that the slope in the regression between temperature and the percentage of Chl *a* in each size class took absolute values of 0.8% $^{\circ}C^{-1}$ and 0.5% $^{\circ}C^{-1}$ for pico- and microphytoplankton, respectively (Table 3). Our simulations (Fig. 6) show that the temperature–size rule can only explain a change in the contribution of these size classes to total biomass of 0.4% and 2.8% for a 10°C change in temperature, or 0.04% $^{\circ}C^{-1}$ and 0.28% $^{\circ}C^{-1}$. This strongly suggests that at least part of the observed correlation between temperature and phytoplankton size structure reflects the effect of other variables that covary with temperature, rather than a direct effect of temperature per se.

Discussion

The hypothesis that temperature per se plays a direct role in controlling the variability of phytoplankton size structure in the ocean must be rejected. Phytoplankton size structure, and in particular the biomass dominance of small vs. large cells, depends on total community biomass and productivity, both of which are mainly controlled by the rate of resource (nutrient and light) utilization, although also affected by advection and mortality. The linkage between high (low) resource utilization rate and a dominance of large (small) cells is independent of temperature (Table 5). When nutrients are in low supply, phytoplankton standing stocks and productivity are low and the community is dominated by small cells, which due to their large surface-area-to-volume ratio are better equipped to avoid nutrient diffusion limitation (Chisholm 1992; Kiørboe 1993). Similarly, if light is limiting, the community will also be dominated by small cells, which, thanks to their smaller package effect, are more efficient at harvesting photons (Sunda and Huntsman 1997; Raven 1998). At all temperatures, when resources are plentiful primary production increases and leads to blooms, which are typically dominated by large cells, diatoms in particular. Diatoms form the bulk of blooms in the ocean because they have several functional traits that favor them over smaller cells under conditions of high and intermittent resource supply (Falkowski and Oliver 2007; Cermeño et al. 2011), including a higher maximal nutrient uptake rate relative to their nutrient minimum quotas (Litchman et al. 2007) and the ability to take up and accumulate nutrients in excess of their immediate requirements (Thingstad et al. 2005). Large size also confers some protection against grazing, and the disparate generation times of large algae and their metazoan grazers provides an additional mechanism to explain the dominance of blooms by microphytoplankton (Kiørboe 1993). All these biophysical and trophic constraints operate in cold, temperate, and warm waters; as shown in Figs. 3, 7, data from different temperature ranges conform to a single, saturating function of total biomass and productivity, which indicates that phytoplankton size structure is independent of temperature.

The commonly observed association between cold (warm) temperature and a dominance of large (small) phytoplankton (Agawin et al. 2000; Marañón et al. 2001; Hilligsøe et al. 2011) stems from the fact that temperature is broadly anti-correlated with nutrient supply in marine

Table 4. Results of multiple regression analysis on the percentage of Chl *a* in each size fraction (picophytoplankton [pico], nanophytoplankton [nano], and microphytoplankton [micro]) using temperature and primary production as independent variables. Partial *T*-values indicate the size of the statistical effect of the independent variable when all other independent variables are considered. Squared semi-partial correlation coefficients indicate the proportion of total variance explained by each independent variable. P_T indicates the probability that a partial *T*-value of equal or greater magnitude would be obtained by chance alone. Primary production data were $\log_{10}$-transformed prior to analysis. In all cases, $n = 165$.

Dependent variable	Independent variable and constant	Coefficient (standard error)	Partial *T*	Squared semi-partial correlation	P_T	r^2	*p*
% pico Chl *a*	Temperature	1.06(0.14)	7.58	0.12	<0.00001	0.65	<0.00001
	Primary production	−25.27(1.56)	−16.23	0.57	<0.00001		
	Constant	51.62(2.72)					
% nano Chl *a*	Temperature	−0.25(0.10)	−2.39	0.03	0.018	0.17	<0.00001
	Primary production	−5.82(1.16)	−5.00	0.13	<0.00001		
	Constant	35.99(2.03)					
% micro Chl *a*	Temperature	−0.81(0.16)	−5.21	0.05	<0.00001	0.67	<0.00001
	Primary production	31.09(1.73)	17.98	0.65	<0.00001		
	Constant	12.38(3.01)					

waters (Kamykowski and Zentara 1986). Thus, a common way to evaluate the possible role of nutrients in controlling phytoplankton size structure has been to take into account nutrient concentration (Agawin et al. 2000; Morán et al. 2010; Hilligsøe et al. 2011). However, at the local scale of many oceanographic surveys, the correlation between nutrient concentration and actual nutrient utilization by phytoplankton is often poor. Nutrient concentrations are often high during periods of low phytoplankton biomass and growth, e.g., winter mixing conditions in temperate and polar ecosystems, when light is limiting. Immediately after a strong injection of nutrients into the euphotic layer, phytoplankton may not yet show any increase in biomass or intrinsic growth rate because their physiological response is subject to a time lag. Conversely, at the peak of a large phytoplankton bloom, nutrient concentrations are always relatively low. Therefore, simply taking into account nutrient distribution does not allow evaluation of the relative role of temperature vs. resources in controlling phytoplankton size structure. Nutrient addition experiments, however, can be used to separate the two factors (Agawin et al. 2000). As we have shown, in situ iron addition experiments in cold, temperate, and warm waters unequivocally demonstrate that, while temperature remains constant, the addition of the limiting nutrient results in a phytoplankton bloom that is always dominated by microphytoplankton (Fig. 5). Irigoien et al. (2005) noted that the key relationship is "not between cell size and nutrients, but between cell size and growth rates or growing conditions." Similarly, our results indicate that when one considers light and nutrients together as a single, aggregate resource, then high rates of resource utilization by phytoplankton are invariably associated with a dominance by large species.

Temperature-driven changes in phytoplankton size structure have been explained (Daufresne et al. 2009; Morán et al. 2010) as a manifestation of the temperature–size rule, which states that, *other factors being equal*, an increase in temperature results in a decrease of mean individual body size within a population (Atkinson et al. 2003). The reasoning is that, if all individuals of the phytoplankton assemblage decrease in cell size as temperature goes up, and given that picoplankton are defined as cells of < 2 μm in diameter, the percentage of biomass accounted by this size class should increase with temperature. However, for protists the temperature–size rule predicts a decrease of only 2.5% in cell volume for each °C of warming (Atkinson et al. 2003), a rate that is too small to account for the changes in phytoplankton size structure and mean cell size observed across temperature gradients. We have shown that a reduction of cell volume of 25% and 50%, associated with a temperature increase of 10°C and 20°C, respectively, only causes very minor changes in phytoplankton size structure (Fig. 6). Morán et al. (2010) reported that the mean picophytoplankton cell size in the eastern North Atlantic, measured throughout the year, decreases from ~ 2 to 0.2 μm^3 with a 10°C increase in temperature. Based on the temperature–size rule, this temperature gradient could at most cause a reduction of 25% in mean picophytoplankton cell volume, compared with the observed 90%. Therefore, most of the observed

Table 5. Temperature, resource utilization rate, and phytoplankton size structure in the ocean. The examples for each situation are taken from the studies cited in Fig. 5 and Table 2.

Temperature	Resource utilization rate	Dominant phytoplankton size	Examples
Warm	Low	Small	Eastern Equatorial Pacific (iron limitation) North and South Atlantic subtropical gyres (macronutrient limitation)
Warm	High	Large	Iron-fertilized patch during IronEx II experiment High-nutrient, coastal waters (Iskenderun Bay, Johor Strait, Tehuantepec Gulf)
Temperate	Low	Small	Ría de Vigo (northwest Iberian peninsula) in winter (light limitation) Eastern subarctic North Pacific in summer (iron limitation)
Temperate	High	Large	Ría de Vigo during the upwelling season (Apr–Jul) Iron-fertilized patch during SERIES experiment
Cold	Low	Small	Southern Ocean HNLC waters in summer (iron limitation) Marguerite Bay (Antarctic peninsula) in winter (light limitation)
Cold	High	Large	Iron-fertilized patch during iron addition experiments in the Southern Ocean Marguerite Bay during the summer phytoplankton bloom

change must have resulted from seasonal changes in the relative abundance of cyanobacteria and picoeukaryotes. In temperate waters, such changes are mainly driven by variability in the degree of mixing and rate of nutrient supply towards the euphotic layer (Calvo-Díaz and Morán 2006). This may also explain why Morán et al. (2010) found a ca. 10-fold difference in mean picophytoplankton cell volume between the eastern and the western North Atlantic for samples with the same temperature (12–14°C). This temperature range corresponds to winter and spring in the eastern region and summer and early autumn in the western region, which are broadly associated with high-mixing, nutrient-rich and low-mixing, nutrient-poor conditions, respectively.

Nutrient availability is also a strong determinant of intraspecific mean cell size in picoautotrophs (DuRand et al. 2001; Calvo-Díaz and Morán 2006), which means that part of the decrease in *Synechococcus* and *Prochlorococcus* mean cell size observed by Morán et al. (2010) as temperature became warmer was probably a consequence of nutrient depletion in the upper mixed layer during the summer stratification period. In any event, although temperature- and nutrient-driven changes in intraspecific population mean cell size may contribute to very minor variations in size structure, they cannot explain the large changes that are observed throughout the ocean, whereby the relative contribution of pico- or microphytoplankton to total biomass may change from $< 5\%$ to $> 90\%$ or vice versa. These changes reflect fundamental reorganizations in the species composition of the assemblage, which result from taxon- and size-dependent differences in key functional traits involved in resource acquisition and use (Litchman et al. 2007; Falkowski and Oliver 2007).

It has been shown that the experimental warming of marine (Sommer and Lengfellner 2008) and freshwater (Yvon-Durocher et al. 2011) plankton assemblages contained in mesocosms can induce a shift towards an increased importance of smaller phytoplankton species, although in this case the underlying mechanism seems to be a temperature-mediated change in grazing pressure upon the different phytoplankton size classes. It is suggested that warming, by stimulating the grazing activity of copepods and ciliates feeding on microphytoplankton, could result in a shift towards an increased dominance of smaller cells (Sommer and Lengfellner 2008). It is unclear, however, why the grazers that feed upon pico- and nanophytoplankton were not stimulated in the warmed treatments, particularly since both ingestion and growth rates of such grazers have been shown to increase with temperature in the range 10–20°C (Montagnes et al. 2008). They may have been prey of the increasingly active copepods, which would result in a trophic cascade leading to the observed shift in phytoplankton size structure. In any case, even if grazing were favoring a shift of phytoplankton size structure towards a growing importance of smaller species as temperature increases, the fact remains that blooms in warm waters are still dominated by microphytoplankton (Figs. 5, 7). In warm (> 25°C), coastal waters affected by anthropogenic inputs, increased total phytoplankton biomass is associated with an increased importance of microphytoplankton (Gin et al. 2000; Polat and Aka 2007). The same trend is present in low-latitude, coastal regions where upwelling and vertical mixing brings nutrients into the euphotic zone but the high incident solar radiation keeps surface temperatures above 25°C (Robles-Jarero and Lara-Lara 1993; Latasa and Bidigare 1998). During the IronEx II experiment in the Equatorial Pacific, when surface-water temperatures were > 25°C, fertilization caused a dramatic change in the phytoplankton community structure, from one dominated by picoplankton to one dominated by large diatoms (Cavender-Bares et al. 1999). It thus seems unlikely that grazing can prevent large phytoplankton from dominating blooms in warm conditions. In fact, the stronger grazing pressure exerted upon the smaller phytoplankton, on account of the similar generation times of prey and predator, may actually contribute to explain the shift towards a dominance of large-sized species during the development of blooms (Kiørboe 1993; Landry et al. 2000; Irigoien et al. 2005).

Elucidating the relative role of temperature and resources, together with mortality, in controlling phytoplankton size structure is important to predict the response of marine pelagic ecosystems to global change. In many coastal regions, even if the sea surface warms, nutrient availability

will continue to increase as a result of growing anthropogenic eutrophication (Seitzinger et al. 2002). The occurrence of coastal blooms as a result of agricultural runoff is expected to increase significantly during the coming decades (Beman et al. 2005). In the case of relatively well mixed coastal areas where silicate is available in excess of nitrate, nitrogen-dominated runoff inputs stimulate phytoplankton growth and biomass and lead a dominance by large-sized diatoms (Del Amo et al. 1997). In the open ocean, surface warming will likely increase the thermal stratification and geographical extent of the subtropical gyres (Polovina et al. 2008), thus exacerbating nutrient limitation, reducing primary production (Behrenfeld et al. 2006) and leading to an increased importance of smaller phytoplankton. By contrast, in high-latitude regions surface warming (together with freshening) will result in reduced vertical mixing, which may enhance primary production in areas where phytoplankton are light-limited (Doney 2006) and thus cause an increased importance of large cells. It has also been shown that freshening-induced stratification leads to reduced nutrient availability for surface phytoplankton in some parts of the Arctic, favoring smaller cells (Li et al. 2009). In conclusion, given that resource availability and not temperature is the key factor explaining the relative success of different algal size classes, no single, universal effect of ocean warming on phytoplankton size structure should be anticipated because the relationship between temperature and resource supply is not the same everywhere. Understanding the effects of global change upon resource availability will be central to predict future alterations in the size structure and associated functional properties of phytoplankton in the ocean.

Acknowledgments

We thank P. W. Boyd, A. Clarke, and A. Tsuda for making their data available. Comments from three anonymous reviewers are gratefully acknowledged. This research was funded by the Spanish Ministry of Science and Technology through the Ciencias y Tecnologías Marinas (CTM) project CTM2008-03999 (Macroecological patterns in marine phytoplankton) to E. M.

References

Agawin, N. S. R., C. M. Duarte, and S. Agustí. 2000. Nutrient and temperature control of the contribution of picoplankton to phytoplankton biomass and production. Limnol. Oceanogr. **45:** 591–600, doi:10.4319/lo.2000.45.3.0591

Atkinson, D., B. J. Ciotti, and D. J. S. Montagnes. 2003. Protists decrease in size linearly with temperature: ca. 2.5% $^{\circ}C^{-1}$. Proc. R. Soc. B **270:** 2605–2611, doi:10.1098/rspb.2003.2538

Behrenfeld, M. J., and others. 2006. Climate-driven trends in contemporary ocean productivity. Nature **444:** 752–755, doi:10.1038/nature05317

Beman, J. M., K. R. Arrigo, and P. A. Matson. 2005. Agricultural runoff fuels large phytoplankton blooms in vulnerable areas of the ocean. Nature **434:** 211–214, doi:10.1038/nature03370

Calvo-Díaz, A., and X. A. G. Morán. 2006. Seasonal dynamics of picoplankton in shelf waters of the southern Bay of Biscay. Aquat. Microb. Ecol. **42:** 159–174, doi:10.3354/ame042159

Cavender-Bares, K. K., E. L. Mann, S. W. Chisholm, M. E. Ondrusek, and R. R. Bidigare. 1999. Differential response of equatorial Pacific phytoplankton to iron fertilization. Limnol. Oceanogr. **44:** 237–246, doi:10.4319/lo.1999.44.2.0237

Cermeño, P., P. Estévez-Blanco, E. Marañón, and E. Fernández. 2005. Maximum photosynthetic efficiency of size-fractionated phytoplankton assessed by ^{14}C-uptake and fast repetition rate fluorometry. Limnol. Oceanogr. **50:** 1438–1446, doi:10.4319/lo.2005.50.5.1438

———, J. B. Lee, K. Wyman, O. Schofield, and P. G. Falkowski. 2011. Competitive dynamics in two species of marine phytoplankton under non-equilibrium conditions. Mar. Ecol. Prog. Ser. **429:** 19–28, doi:10.3354/meps09088

Chisholm, S. W. 1992. Phytoplankton size, p. 213–237. *In* P. G. Falkowski and A. D. Woodhead [eds.], Primary productivity and biogeochemical cycles in the sea. Plenum Press.

Daufresne, M., K. Lengfellner, and U. Sommer. 2009. Global warming benefits the small in aquatic ecosystems. Proc. Natl. Acad. Sci. USA **106:** 12788–12793, doi:10.1073/pnas.0902080106

Del Amo, Y., B. Queguiner, P. Treguer, H. Breton, and L. Lampert. 1997. Impacts of high-nitrate freshwater inputs on macrotidal ecosystems. II. Specific role of the silicic acid pump in the year-round dominance of diatoms in the Bay of Brest (France). Mar. Ecol. Prog. Ser. **161:** 225–237, doi:10.3354/meps161225

Doney, S. C. 2006. Plankton in a warmer world. Nature **444:** 695–696, doi:10.1038/444695a

DuRand, M. D., R. J. Olson, and S. W. Chisholm. 2001. Phytoplankton population dynamics at the Bermuda Atlantic Time-series station in the Sargasso Sea. Deep-Sea Res. II **48:** 1983–2003, doi:10.1016/S0967-0645(00)00166-1

Falkowski, P. G., R. T. Barber, and V. Smetacek. 1998. Biogeochemical controls and feedbacks on ocean primary production. Science **281:** 200–206, doi:10.1126/science.281.5374.200

———, and M. J. Oliver. 2007. Mix and match: How climate selects phytoplankton. Nature Rev. Microbiol. **5:** 813–819.

Finkel, Z. V., J. Beardall, K. Flynn, A. Quigg, T. A. V. Rees, and J. A. Raven. 2010. Phytoplankton in a changing world: Cell size and elemental stoichiometry. J. Plankton Res. **32:** 119–137, doi:10.1093/plankt/fbp098

Gin, K. Y. H., X. Lin, and S. Zhang. 2000. Dynamics and size structure of phytoplankton in the coastal waters of Singapore. J. Plankton Res. **22:** 1465–1488, doi:10.1093/plankt/22.8.1465

Hilligsøe, K. M., K. Richardson, J. Bendtsen, L. L. Sørensen, T. G. Nielsen, and M. M. Lyngsgaard. 2011. Linking phytoplankton community size composition with temperature, plankton food web structure and sea-air CO_2 flux. Deep-Sea Res. I **58:** 826–838, doi:10.1016/j.dsr.2011.06.004

Irigoien, X., K. J. Flynn, and R. P. Harris. 2005. Phytoplankton blooms: A 'loophole' in microzooplankton grazing impact? J. Plankton Res. **27:** 313–321, doi:10.1093/plankt/fbi011

Irwin, A. J., and Z. V. Finkel. 2008. Mining a sea of data: Deducing the environmental controls of ocean chlorophyll. PLoS ONE **3:** e3836, doi:10.1371/journal.pone.0003836

Kamykowski, D., and S. J. Zentara. 1986. Predicting plant nutrient concentrations from temperature and sigma-*t* in the upper kilometer of the world ocean. Deep-Sea Res. I **33:** 89–105.

Kiørboe, T. 1993. Turbulence, phytoplankton cell size, and the structure of pelagic food webs. Adv. Mar. Biol. **29:** 1–72, doi:10.1016/S0065-2881(08)60129-7

Landry, M. R., and others. 2000. Biological response to iron fertilization in the eastern equatorial Pacific (IronEx II). I. Microplankton community abundances and biomass. Mar. Ecol. Prog. Ser. **201:** 27–42, doi:10.3354/meps201027

Latasa, M., and R. M. Bidigare. 1998. A comparison of phytoplankton populations of the Arabian Sea during the Spring Intermonsoon and Southwest Monsoon of 1995 as described by HPLC-analyzed pigments. Deep-Sea Res. II **45:** 2133–2170, doi:10.1016/S0967-0645(98)00066-6

Legendre, L., and F. Rassoulzadegan. 1996. Food-web mediated export of biogenic carbon in oceans. Mar. Ecol. Prog. Ser. **145:** 179–193, doi:10.3354/meps145179

Li, W. K. W., F. A. McLaughlin, C. Lovejoy, and E. C. Carmack. 2009. Smallest algae thrive as the Arctic Ocean freshens. Science **326:** 539, doi:10.1126/science.1179798

Litchman, E., C. A. Klausmeier, O. M. Schofield, and P. G. Falkowski. 2007. The role of functional traits and trade-offs in structuring phytoplankton communities: Scaling from cellular to ecosystem level. Ecol. Lett. **10:** 1170–1181, doi:10.1111/j.1461-0248.2007.01117.x

Marañón, E., P. Cermeño, J. Rodríguez, M. V. Zubkov, and R. P. Harris. 2007. Scaling of phytoplankton photosynthesis and cell size in the ocean. Limnol. Oceanogr. **52:** 2190–2198, doi:10.4319/lo.2007.52.5.2190

———, P. M. Holligan, R. Barciela, N. González, B. Mouriño, M. J. Pazó, and M. Varela. 2001. Patterns of phytoplankton size-structure and productivity in contrasting open ocean environments. Mar. Ecol. Prog. Ser. **216:** 43–56, doi:10.3354/meps216043

Montagnes, D. J. S., G. Morgan, J. Bissinger, D. Atkinson, and T. Weisse. 2008. Short-term temperature change may impact freshwater carbon flux: A microbial perspective. Global Change Biol. **14:** 1–16, doi:10.1111/j.1365-2486.2008.01700.x

Morán, X. A. G., A. López-Urrutia, A. Calvo-Díaz, and W. K. W. Li. 2010. Increasing importance of small phytoplankton in a warmer ocean. Global Change Biol. **16:** 1137–1144, doi:10.1111/j.1365-2486.2009.01960.x

Polat, S., and A. A. Aka. 2007. Total and size fractionated phytoplankton biomass off Karataş, north-eastern Mediterranean coast of Turkey. J. Black Sea/Mediterr. Environ. **13:** 191–202.

Polovina, J. J., E. A. Howell, and M. Abecassis. 2008. Ocean's least productive waters are expanding. Geophys. Res. Lett. **35:** L03618, doi:10.1029/2007GL031745

Raven, J. A. 1998. Small is beautiful: The picophytoplankton. Funct. Ecol. **12:** 503–513, doi:10.1046/j.1365-2435.1998.00233.x

Reul, A., and others. 2005. Variability in the spatio-temporal distribution and size structure of phytoplankton across an upwelling area in the NW-Alboran Sea (W-Mediterranean). Cont. Shelf Res. **25:** 589–608, doi:10.1016/j.csr.2004.09.016

Robles-Jarero, E. G., and J. R. Lara-Lara. 1993. Phytoplankton biomass and primary productivity by size classes in the Gulf of Tehuantepec, Mexico. J. Plankton Res. **15:** 1341–1358, doi:10.1093/plankt/15.12.1341

Seitzinger, S. P., C. Kroeze, A. F. Bouwman, N. Caraco, F. Dentener, and R. V. Styles. 2002. Global patterns of dissolved inorganic and particulate nitrogen inputs to coastal systems: Recent conditions and future projections. Estuaries **25:** 640–655, doi:10.1007/BF02804897

Sommer, U., and K. Lengfellner. 2008. Climate change and the timing, magnitude, and composition of the phytoplankton spring bloom. Global Change Biol. **14:** 1199–1208, doi:10.1111/j.1365-2486.2008.01571.x

Sunda, W. G., and S. A. Huntsman. 1997. Interrelated influence of iron, light and cell size on marine phytoplankton growth. Nature **390:** 389–392, doi:10.1038/37093

Thingstad, T. F., L. Øvreås, J. K. Egge, T. Løvdal, and M. Heldal. 2005. Use of non-limiting substrates to increase size; a generic strategy to simultaneously optimize uptake and minimize predation in pelagic osmotrophs? Ecol. Lett. **8:** 675–682, doi:10.1111/j.1461-0248.2005.00768.x

Yvon-Durocher, G., J. M. Montoya, V. Trimmer, and G. Woodward. 2011. Warming alters the size spectrum and shifts the distribution of biomass in freshwater ecosystems. Global Change Biol. **17:** 1681–1694, doi:10.1111/j.1365-2486.2010.02321.x

Associate editor: Heidi M. Sosik

Received: 02 February 2012
Accepted: 14 May 2012
Amended: 16 May 2012